



Enhancing mechanical, thermo-mechanical and low velocity impact properties of epoxy methyl ricinoleate toughened epoxy composites by integrating microcrystalline cellulose

Sathyaraj Sankar lal · Sekar Kannan

Received: 28 January 2024 / Accepted: 16 May 2024 / Published online: 28 May 2024
© The Author(s), under exclusive licence to Springer Nature B.V. 2024

Abstract Flax fibre-reinforced bio-composites are developed using both unmodified petroleum-based epoxy and Epoxy Methyl Ricinoleate (EMR) toughened epoxy modified with microcrystalline cellulose (MCC) as the base matrix. Base-catalyzed transesterification is employed for the synthesis of EMR as a low-viscosity reactive green monomer for the modification of petroleum-based epoxy. MCC is incorporated into the EMR-modified epoxy through mechanical stirring and subsequent sonication at loading rates of 1%, 3%, and 5% by weight. The compression molding technique was employed to prepare the composites. The results show an enhancement in tensile strength, modulus, impact strength, and inter-laminar shear strength values up to 19%, 34%, 34.2%, and 22.7%, respectively for MCC filled EMR toughened epoxy composite compared to neat epoxy composite. The storage and loss moduli, as revealed by the dynamic mechanical analysis (DMA), also demonstrate improvement for the 3% MCC-C composite signifying the improved fibre/matrix bonding. The low-velocity impact test at 10 J and 20 J for non-perforation and perforation conditions was also performed on the composites. The MCC-incorporated EMR-modified composite demonstrated the highest

low velocity impact resistance among all other bio-composites, highlighting its potential for use in semi-structural applications due to the enhanced interfacial adhesion. The SEM analysis revealed that the fibre surface of MCC-modified EPEMR20 composites exhibited surface damage, and adherence of MCC fillers and matrix fragments, indicating superior adhesion to the matrix system.

Keywords Epoxy Methyl Ricinoleate · Castor oil · Low Velocity Impact Test · Microcrystalline Cellulose · Mechanical Properties · Viscoelastic Properties · Bio composites

Introduction

The utilization of fibre-reinforced polymeric composite (FRPC) materials has witnessed substantial growth over the past few decades across various technical domains. Fibre reinforced polymer composites (FRPCs) outperform metals and alloys in terms of specific strength and modulus, fatigue performance, reduced thermal expansion, greater corrosion resistance, and more (Di Mauro et al. 2021; Sankar lal et al. 2022a). FRPCs offer unique properties that can be customized to meet specific requirements through careful selection of fiber and polymer blends. Material engineers can leverage a vast range of design choices to develop composites suitable for various applications, spanning from aerospace to sports equipment,

S. Sankar lal (✉) · S. Kannan
Materials Science Laboratory, Department of Mechanical Engineering, National Institute of Technology Calicut, Kozhikode, Kerala 673601, India
e-mail: sathyaraj_p190085me@nitc.ac.in

both in structural and non-structural domains (Sankar Lal et al. 2022a; Sankar Lal et al. 2023). Synthetic fiber composites are increasingly favored for their notable attributes such as strength, impact resistance, durability, and chemical stability. Nonetheless, growing environmental apprehensions and the quest for sustainability offer an intriguing chance to cultivate eco-friendly materials. This emphasizes the significance of incorporating renewable resources into product design (Mahboob et al. 2017).

The growing environmental concerns have resulted in a shift towards incorporating natural materials as substitutes for synthetic fibres, such as carbon, glass, or kevlar fibres, in composites that incorporate both thermosetting and thermoplastic polymers. Epoxy resin is unique among thermoset polymers because of its high rigidity, great chemical resistance, improved dimensional stability, minimum curing shrinkage, and low expansion coefficient. However, it confronts a number of problems, including brittleness, high cost, non-biodegradability, and health hazards (Sankar Lal et al. 2022b). Hence, ongoing scientific research prioritizes replacing petrochemical materials with renewable, bio-based alternatives. These resources present a viable option for substituting petroleum-based polymers, either partially or entirely, in a sustainable manner. The major objective is to create bio-based polymers that are both cost-effective and environmentally friendly, while also surpassing the performance of existing polymers. Plant oils, abundant in unsaturated triglycerides, are ideal for producing polymer precursors due to their chemical versatility. However, it's crucial to note that utilizing bio-based sources doesn't automatically ensure biodegradability.

The presence of hydroxy groups in castor oil has sparked growing interest in castor oil-based bio-resins within the field of bio-based polymers. These hydroxy groups offer versatility by enabling chemical modifications to introduce various functionalities or crosslinking sites. Consequently, they enhance the diversity of polymers derived from castor oil (Fu et al. 2020; Kannan and Sankar Lal 2023). Moreover, when employed as a matrix, these hydroxy groups may form hydrogen bonding with natural fiber cellulose. This could enhance interfacial adhesion without necessitating chemical modification of the fibers, thereby reducing the need for additional processes to achieve improved characteristics (Sankar

lal et al. 2022a; Sankar Lal et al. 2023). Moreover, given the inedibility of castor oil, its use in the polymer sector would not pose a threat to the food market or the global supply of edible oils (Paluvai et al. 2015; Sudha et al. 2017a). Recently, it has become possible to successfully manufacture epoxidized oils and esterified epoxidized oils. Several authors have reported using epoxidized castor oil (ECO) for its toughening capabilities in epoxy blends (Sudha et al. 2017b; Sankar Lal et al. 2022b). Similarly, Sankar Lal et al. (2022b) reported the synthesis of esterified castor oil-based epoxy blends with improved characteristics due to their decreased viscosity, which results in better interaction with the hardener system. Prior study has shown that incorporating a plant oil-based bio-resin boosted matrix toughness; nevertheless, it dramatically degraded the mechanical and thermo-physical properties of the original polymer. (Sahoo et al. 2015a, 2018a; Kumar et al. 2018; Sankar Lal et al. 2022b; Sankar and Sekar 2023). The drawbacks of bio-epoxy can be mitigated by modifying it with nano or micro fillers. In polymer technology, adding these fillers to bio-based polymer systems is crucial for improving thermal stability, raising the glass transition temperature, and increasing dimensional stability. Various fillers like carbon nanotubes, clays, carbonaceous fillers, metallic particles, and aramid pulp are used to enhance resin properties. However, challenges such as production costs and dispersion issues persist. Nonetheless, there is increasing interest in organic and bio-fillers for eco-friendly composites across industries (Ramesh et al. 2020; Kerche et al. 2021; Motta Neves et al. 2021). Cellulose, extracted from various plant sources, including forms like cellulose nano-fibres (CNFs), cellulose nanocrystals (CNCs), microcrystalline cellulose (MCC), and micro-fibrillated cellulose (MFC) stands as the amplest biopolymer on earth among bio-fillers (Nascimento et al. 2021; Motta Neves et al. 2021). However, bio-epoxies modified with the ideal quantity of MCC may not possess adequate strength for use in industrial applications and hence should be reinforced with continuous fibres.

Fiber-reinforced polymer composites, known for their exceptional strength and modulus, are extensively utilized in wind energy, automotive, and aerospace industries. These sectors require lightweight materials to comply with regulations aimed at reducing carbon dioxide emissions, especially

in automotive manufacturing (Sahoo et al. 2018b). Thus, the objective is to incorporate thermosetting matrices sourced from bio-materials into the production of entirely green and sustainable materials, utilizing bio-based materials for both the matrix and reinforcement. In this context, flax fiber emerges as a widely used and cost-effective bast natural fiber globally (Prasad et al. 2018). Its high specific mechanical properties are attributed to its excellent mechanical characteristics, featuring a specific strength of 1300 MPa/gcm⁻³ and a tensile modulus of 20 GPa. These properties are comparable to those of glass fibres, which have a specific strength of 1350 MPa/gcm⁻³ and a modulus of 30 GPa (Prasad et al. 2020; Sankar Lal et al. 2022a; Sankar Lal et al. 2023).

In our prior study, we addressed the issues for moduli loss, dimensional, and thermal stability in toughened 20% EMR/epoxy copolymer by incorporating rigid MCC fillers (Sankar and Sekar 2023). However, to enhance its performance for potential industrial applications, further improvement is crucial. Integrating continuous fibers presents a promising avenue for this enhancement. Previous research has explored the utilization of cellulose particles in producing hybrid composites with plant fibers, demonstrating its feasibility. Jabbar et al. (2017), for instance, demonstrated that applying a nano-cellulose coating to woven jute fabric enhances the fracture toughness, flexural properties, tensile and storage modulus of the composite with bio-epoxy as the matrix. They also observed a decrease in tensile strength and a reduction in the height of the tan delta peak. Additionally, Parveen et al. (2017) investigated the beneficial impact of using MCC as reinforcement in cementitious composites. The positive effects of MCC on tensile, flexural, and impact strength of alkali treated jute fibre reinforced epoxy composites were documented by Rehman et al. (2019). However, the effect of MCC on the EMR modified epoxy composites has not been explored till date.

In our current study, we aimed to develop a multi-scale hybrid bio-composite to investigate the impact of MCC dispersion on the properties of flax fiber embedded EMR-modified epoxy composites. MCC, with its abundant surface area and hydroxy groups, is expected to form hydrogen bonds with the EMR/epoxy copolymer and flax fiber, enhancing interfacial adhesion. Specifically, the response of multi-scale composites to low-velocity impact (LVI) loads has

not been thoroughly explored, despite recent research on composites using conventional epoxy materials and natural fiber reinforcements. Apart from LVI testing, the composites underwent comprehensive characterization, including assessments of properties at the fiber/matrix interface, tensile strength, impact resistance, and dynamic mechanical behavior.

Experimental

Materials

The epoxy resin employed in the study is based on diglycidyl ether of bisphenol A (DGEBA), with an Epoxy Equivalent Weight (EEW) ranging from 186 to 190 g/mol. The crosslinking agent employed for room temperature curing was based on Triethylenetetramine (TETA). These materials were sourced from Fine Finish Pvt. Ltd., Mumbai, India. Additionally, eco-friendly Epoxidized Castor Oil (ECO) utilized for the synthesis of EMR, was obtained from Jayanth Agro in Mumbai, India. For the transesterification reaction, sodium methoxide and methanol were supplied by M/s Avra Pvt. Ltd, Hyderabad, India. Microcrystalline cellulose was procured from Sigma Aldrich, Bangalore, India. The reinforcement material employed in the study consisted of flax fabric with fibre yarns arranged in a bi-directional plain weave with orientations at 0° and 90°. This flax fabric was sourced from DLS Traders, Tamil Nadu, India. The important properties of epoxy resin, hardener, bio-resins, and reinforcements provided by the suppliers have been enlisted in Table 1 and the chemical structure is shown in Fig. 1.

Synthesis of EMR from ECO

EMR was synthesized from ECO by base-catalyzed transesterification, as detailed in our prior work (Sankar Lal et al. 2022b). In brief, 100 g of ECO were placed in a 250 mL glass beaker on a hot plate with a magnetic stirrer. A solution containing 1 wt.% of sodium methoxide catalyst in 0.030 L of methanol solvent was gradually added to the ECO and stirred at 500 rpm. The reaction was kept at 50 °C for 2 h. Afterwards, the mixture was moved to a separatory funnel to allow glycerol to settle at the bottom. Glycerol was then extracted, resulting in the formation

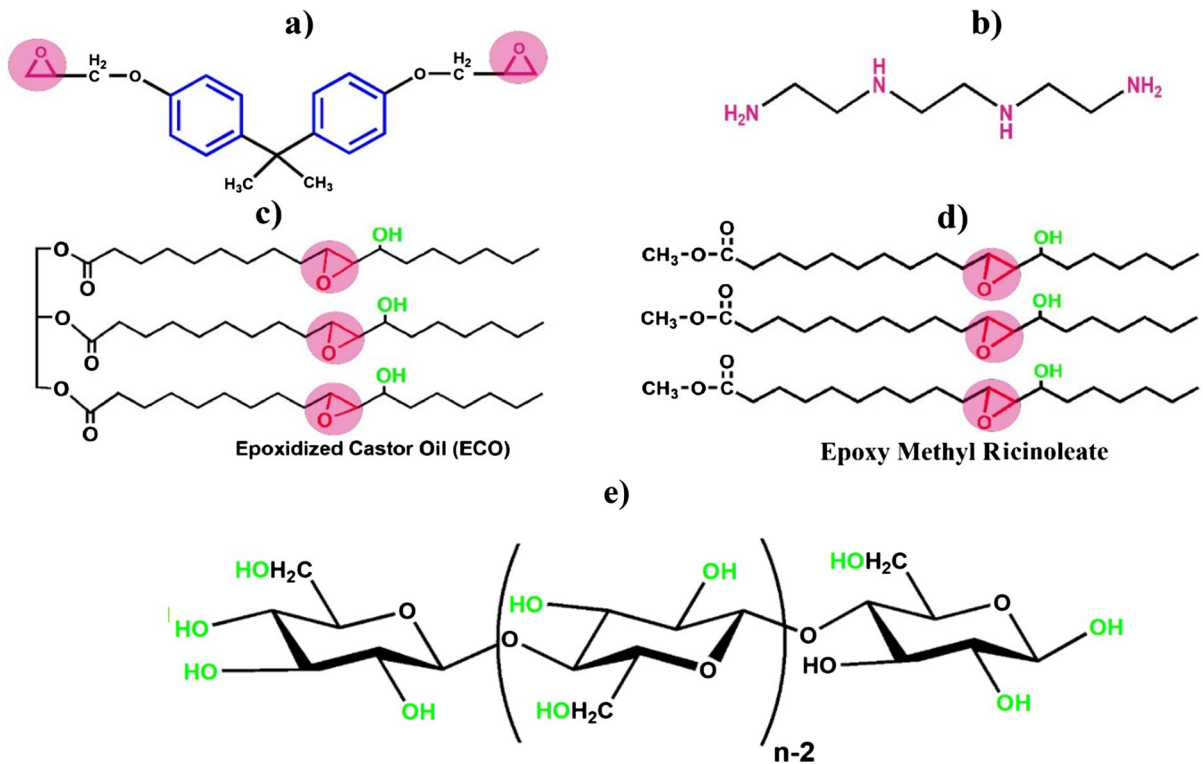


Fig. 1 Chemical structure of **a** DGEBA based epoxy, **b** TETA hardener, **c** ECO, **d** EMR, and **e** MCC

of EMR. The remaining methanol in the EMR was removed using a rotary evaporator. Scheme 1 illustrates the synthesis reaction. The synthesis process was carried out thrice and the epoxy content of EMR was calculated according to standard ASTM D1652 – 11. The epoxy content of EMR was found to be 484 ± 2 g/eq.

Dispersion of MCC in EMR/Epoxy blend

The problem of brittleness in the epoxy matrix was addressed by blending EMR bio-resin with the epoxy resin at various weight ratios. Our prior study (Sankar Lal et al. 2022b) revealed that a 20% EMR blend provided the best stiffness-to-toughness balance, thus chosen for MCC/flax hybrid bio-composite fabrication. The epoxy was blended with EMR bio-resin in an optimized ratio of 80:20 through mechanical stirring at 1000 rpm. This blending process was followed by ultrasonication for a duration of 30 min. The MCC

was introduced into the blend system at varying proportions (1, 3, and 5%) and stirred at 1000 rpm for 1 h. Subsequently, an ultrasonication process was employed for 30 min using a 30-s ON/OFF pulse mode at a frequency of 20 kHz and a power of 180 W. This process aimed to enhance the dispersion of MCC fillers within the system. Afterward, the MCC added blend was degassed in a vacuum oven to remove trapped air bubbles, cooled to room temperature. Subsequently, the hardener was introduced into the resin blend/MCC mixture through a gentle stirring process. The amount of hardener added was found using Eq. 1 and 2. The resulting mixture was then utilized to manufacture hybrid composites.

$$EEW \text{ of blend} = \frac{\text{Total Wt. of mixture}}{\frac{\text{Wt. of resin 1}}{EEW \text{ of resin 1}} + \frac{\text{Wt. of resin 2}}{EEW \text{ of resin 2}}} \quad (1)$$

$$\text{Quantity of hardener} = \frac{AHEW \times \text{Weight of blend}}{EEW \text{ of blend}} \quad (2)$$

Preparation of EMR/Epoxy hybrid biocomposites

To start, the bi-directionally plain woven flax fabric (0/90 orientation) underwent drying in a 75 °C oven for 7 h to eliminate moisture. A releasing agent was applied to the mould to facilitate the easy removal of the composite laminates. The composites were produced by applying a resin and hardener system onto the flax fabric. Seven layers of fabric, wetted with resin, were stacked one over the other. To ensure thorough and uniform wetting of the fibres by the resin, the fibre layers were rolled over with a steel brush. Following this, the mould was sealed and subjected to a constant 150 kgf weight on the top plate, allowing the composite to cure at room temperature for 24 h. Post-curing was performed at 100 °C and 150 °C for 2 h each. The specimens were labeled as Epoxy-C, EPEMR20-C, 1% MCC-C, 3% MCC-C, and 5% MCC-C, representing unmodified epoxy composites, 20% EMR/epoxy blend composite, and various weight percentages of MCC-filled EPEMR20 composites, respectively.

Characterizations

Mechanical characterizations

Specimens for assessing various mechanical properties of Epoxy-C, EPEMR20-C, and their MCC-modified bio-based composites were prepared following ASTM standards. Specifically, for the tensile test, samples with measurements of 250×25×3 mm³ were accurately cut in accordance with the guidelines outlined in ASTM D3039. The evaluation was performed utilizing a UTM (3382 M/s Lloyd Instruments, UK) with a crosshead speed of 1mm/min. Additionally, the impact strength of all samples was analysed using the impact tester (Tinuous olesan, UK), following the guidelines in accordance with the ASTM D256 standard. The test was carried out at an impact velocity of 3.4581 m/s. A specimen with measurements of 63.5×13×3 mm³, featuring a 45° notch depth of 2.54 mm was employed. For each test, five specimens from each set were utilized.

The analysis of interlaminar shear strength (ILSS) employed the short beam shear (SBS) method in accordance with the ASTM D2344-16 standard. The ILSS investigation utilized a three-point bending test

setup with width to thickness and span-to-thickness ratios of 2:1 and 4:1 respectively. Tests were performed on a UTM with a crosshead speed of 1 mm/min. The specimens for testing had dimensions of 18 mm (l)×6 mm (b)×3 mm (h). The ILSS was calculated using Eq. 3.

$$ILSS = \frac{0.75 \times F_{max}}{b \times h} \quad (3)$$

where, F_{max} is the maximum force attained before load drop in N, 'b' is the width of the sample, 'h' is the thickness of the sample. The experiment was repeated five times for each set, and the average values have been reported.

Scanning electron microscopy

Scanning electron microscopy (SEM) was utilized to examine the impact of EMR and MCC particles on the interfacial adhesions of matrix and fibre and also to study failure mode of both the tensile and impact fractured specimens. The investigations were carried out using a Field Emission Scanning Electron Microscope (FE-SEM) SIGMA 300 from Carl Zeiss, Germany, operating at an acceleration voltage of 2.0 kV with an 8.8 mm working distance. To make the surface conductive, a 4 nm thin layer of uniform gold coating was applied to the fractured surface using Quorum Q150T ES equipment. The specimens were cooled before conducting the study.

Dynamic mechanical analysis

The viscoelastic properties of Epoxy-C, EPEMR20-C, and its MCC-modified bio-based composites were examined using the dynamic mechanical analyzer (DMA7100, HITACHI, Japan). The analysis was conducted at a strain rate of 0.09% and a frequency of 1 Hz. The specimens, with dimensions of 63.5×13×3 mm³, underwent heating from room temperature to 180 °C at a rate of 10 °C/min in 3-point bending mode. The test was repeated five times for each set, and the average values have been reported.

Low velocity impact test

The investigation of the non-penetrating and penetrating low velocity impact response of composite

laminates was carried out using a Fractovis drop weight impact tester equipped with an environmental chamber, as illustrated in Fig. 2. A hemispherical steel impactor tup, measuring 12.7 mm in diameter and weighing 1.926 kg, was used to impact the specimens. The clamping system, with an outer diameter of 110 mm, inner diameter of 40 mm, with a clamping force of 500 N held the specimens. The impact tests were conducted at an ambient temperature of 30 °C, with impact energies of 10 J and 20 J for the non-perforation and perforation tests, respectively. During the impact tests, parameters like impact force, impact energy, and deformation were measured and recorded. The drop weight test was conducted five times for each set, and the resulting average values have been documented.

Results and discussion

Characterization of microcrystalline cellulose

To investigate the morphology and size distribution of MCC, scanning electron microscopy (SEM) was utilized (Fig. 3a). The SEM images depicted MCC particles with irregular rod-like shapes, displaying average axial diameters within the 20 to 25 µm range, as indicated in Fig. 3c). Additionally, the elemental composition of MCC was analysed using Energy

Dispersive X-ray Spectroscopy (EDS), revealing the presence of carbon (C) and oxygen (O) elements (Fig. 3b), indicating its untreated state.

Tensile test

The tensile stress–strain curve and properties of all bio-composites are depicted in Fig. 5 and listed in Table 2 respectively. Introducing 20% EMR into Epoxy-C resulted in a 6.4% increase in tensile strength. This improvement stems from enhanced bonding between fibers and the matrix, facilitated by EMR's lower viscosity, enabling more efficient stress transfer from the matrix to the fibers. Conversely, the tensile modulus of EPEMR20-C is reduced compared to Epoxy-C due to decreased rigidity and lower crosslinking density in the flexible EMR-based epoxy blend (Sankar Lal et al. 2023). The addition of MCC fillers resulted in significant improvements in both tensile strength and modulus, with increases of up to 11.74% and 40%, respectively, observed for a 3% MCC content. This enhancement in the tensile properties of EPEMR20-C composites was attributed to the enhanced interaction between the fibers and the matrix facilitated by MCC particles. The large surface area and presence of hydroxy groups in both flax fibers and MCC allowed for the formation of hydrogen bonds, not only between them but also with the hydroxy and carbonyl groups present in EMR

Fig. 2 **a** Fractovis drop-weight tower, **b** Interior view of drop-weight tower, **c** Impactor with load cell, and **d** Sample holder in environment chamber

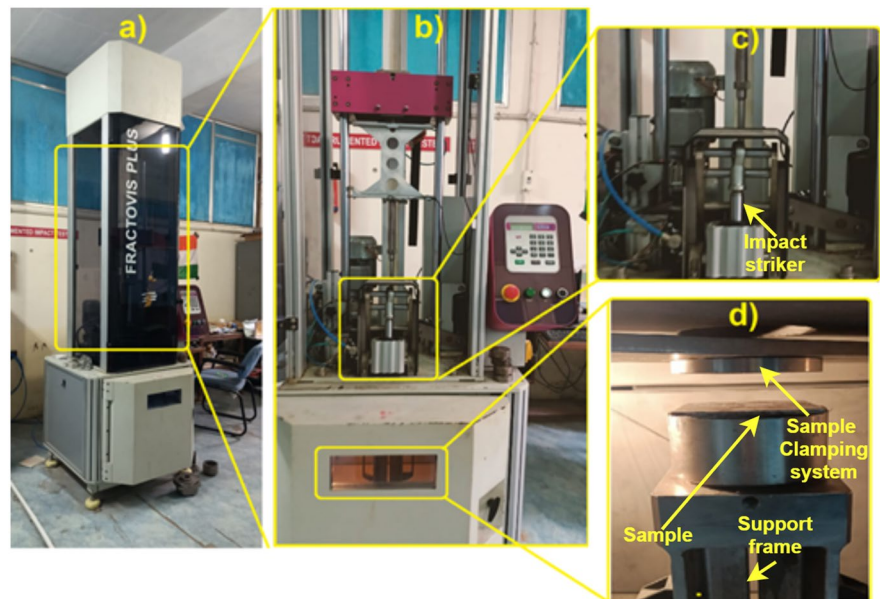


Fig. 3 a SEM morphology, b EDS, and c particle size distribution of MCC

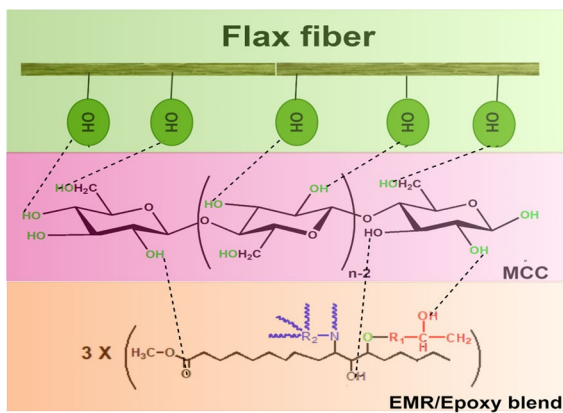
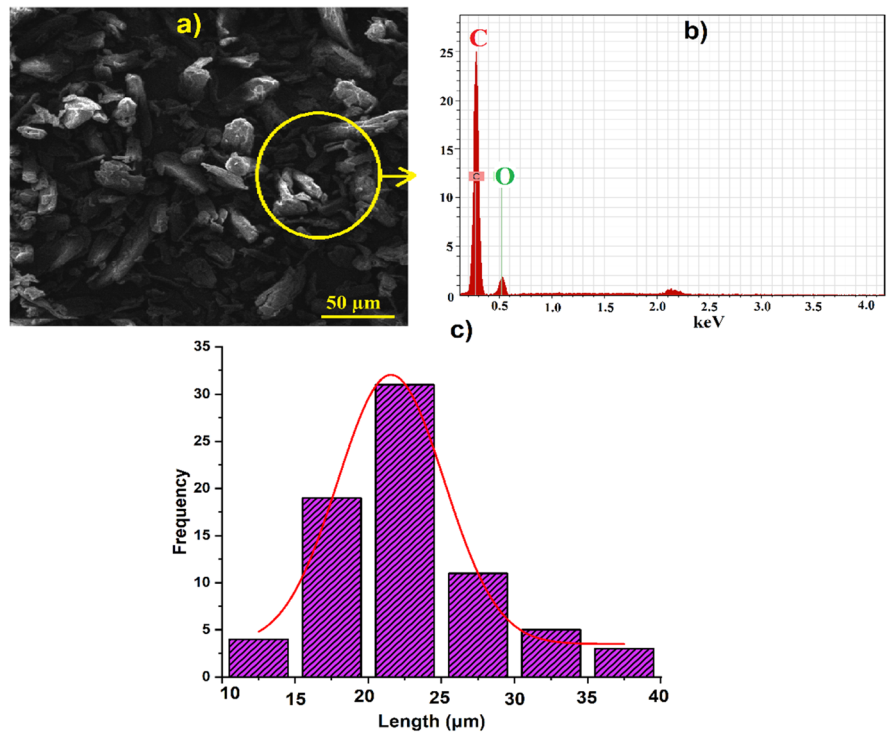


Fig. 4 Systematic representation of chemical bonding between flax fibre, MCC and EMR/epoxy blend

(Stanley et al. 2021). Figure 4 systematically illustrates bond formation. SEM images of the fractured surface reveal chemical interaction between flax fiber and MCC, with MCC particles visibly adhering to the fiber's surface. This bond formation potentially hindered fiber extraction or pullout from the matrix by providing mechanical interlocking when axial tensile loads were applied.

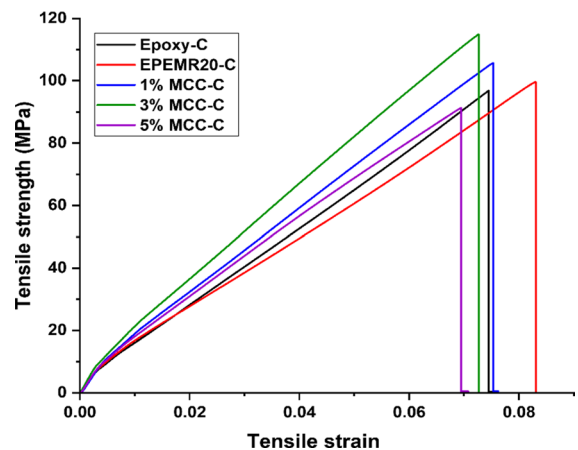


Fig. 5 Tensile stress strain curve of Epoxy-C, EPEMR20-C and its MCC modified composites

Additionally, the flax fabric comprises two interlaced sets of yarns with inherent pores. During composite manufacturing, these pores are filled with a polymer epoxy matrix. Under external loads, the composite experiences a failure process triggered by the formation of micro-cracks originating from regions rich in matrix material (Rehman et al. 2019; Neves et al.

2020). Once a fracture begins, it continues indefinitely, leading to composite failure. However, incorporating MCC fillers into the epoxy matrix can slow down crack propagation, allowing for more energy absorption before ultimate fracture. However, a decrease in tensile properties is observed when the MCC particle content is increased beyond 3%. As indicated by the SEM morphology analysis, this performance decline may be attributed to the increased viscosity of the resin system, which results in the formation of cavities and insufficient interfacial adhesion between the matrix and the fibres (Rehman et al. 2019).

The elongation at break percentage of the neat epoxy composite increased by incorporating 20% EMR, likely due to the aliphatic flexible groups present in EMR bio-resin. However, it decreased upon the addition of MCC fillers, indicating enhanced stiffness of the composite due to a resilient network formed between MCC, flax fiber, and the EPEMR20 resin matrix. This decrease in elongation is attributed to reduced flexibility in the stiff interphase between the filler and the matrix material, resulting in a decline in the plastic deformation region (Sankar and Sekar 2023).

Impact test

Figure 6 illustrates the impact of MCC filler on the impact strength of EPEMR20-C. The impact strength of fiber-reinforced polymer composites is influenced by factors such as the matrix's impact strength, matrix/fiber interfacial adhesion, fiber orientations, and the strength of the reinforced fiber (Prasad et al. 2018; Sahoo et al. 2018b). The Epoxy-C exhibited the lowest impact strength due to poor fiber/matrix adhesion, evidenced by interfacial gaps, and the brittle nature of the epoxy matrix, as indicated by the glossy appearance in fractography (Fig. 7 a)). Incorporating 20% EMR into Epoxy-C led to a significant increase of approximately 12.7% in impact strength. This improvement can be attributed to the less viscous and highly reactive nature of EMR, which reduced the overall viscosity of the resin system. Additionally, EMR created tiny spherical nanoscale cavities that were evenly distributed throughout the matrix phase, as observed in SEM morphology (Fig. 7 b)). This uniform dispersion facilitated shear yielding across the matrix, ultimately enhancing the toughness of the EPEMR20 matrix. The size distribution of these

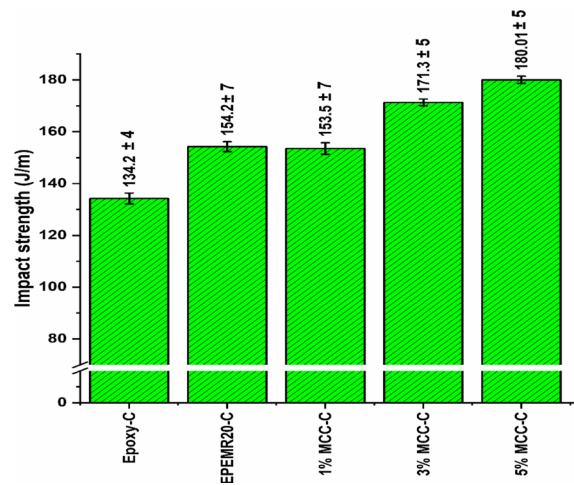
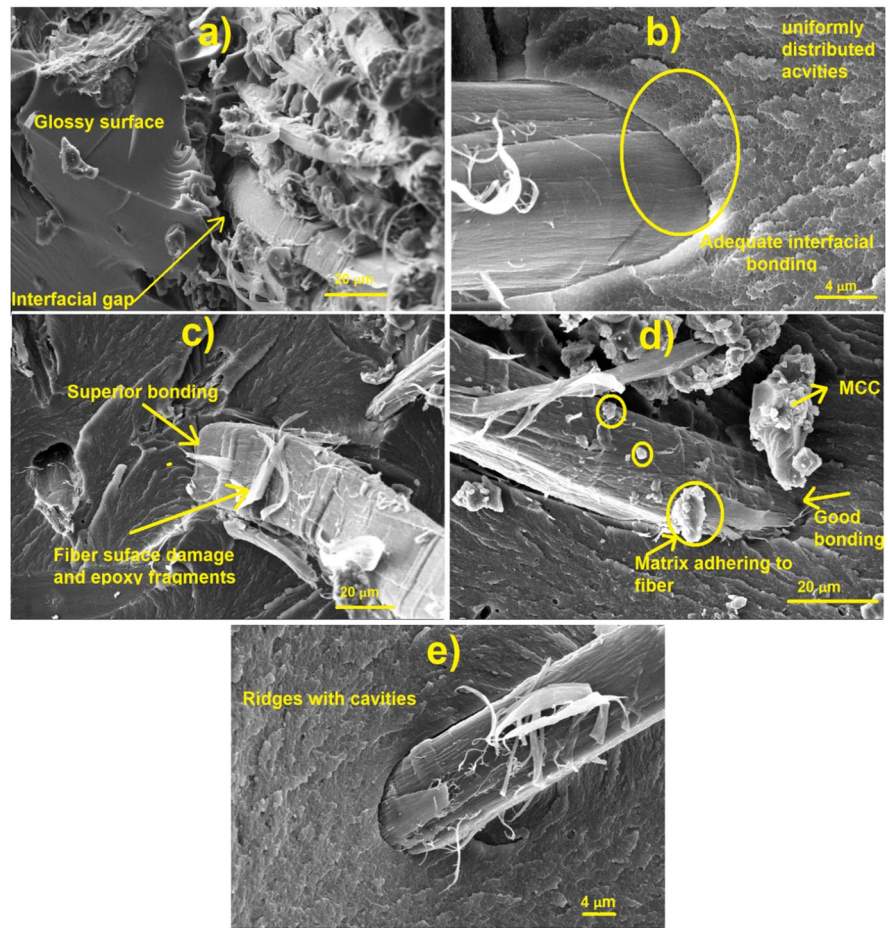


Fig. 6 Effect of MCC fillers on the impact strength of EPEMR20-C composites

cavities plays a crucial role in reinforcing the epoxy network, and their consistent size and distribution contribute to the toughening of the matrix, as previously documented (Sahoo et al. 2015b). This toughening effect of EPEMR20 complemented with improved bonding between the fibre and the matrix, resulted in superior impact strength of the composites.

Adding MCC to EPEMR20-C initially caused a slight decrease in impact strength (at 1% MCC), followed by a gradual increase. Adding MCC to EPEMR20-C initially caused a slight decrease in impact strength (at 1% MCC), followed by a gradual increase. This initial decrease is likely due to the restrictive effect on polymeric chain mobility in EPEMR20 by rigid MCC particles, along with improved adhesion between flax fibers and the EPEMR20 matrix, facilitated by uniform MCC distribution (Pichandi et al. 2018; Sankar and Sekar 2023). With a further increase in MCC content, the impact strength of EPEMR20-C increased by 16.8% for 5% MCC. Prior evidence substantiates the formation of covalent bonds between nanocellulose fibrils and epoxy molecules (Ansari et al. 2016; Pichandi et al. 2018). A similar phenomenon might occur between MCC and epoxy molecules. Furthermore, the hydroxy groups in the polymer backbones of flax fibers and MCC could promote hydrogen bond formation between them. Thus, within the hybrid composites, a resilient network of flax fibers, MCC, and EPEMR20 emerged, effectively preventing flax fiber

Fig. 7 SEM fractography for impact tested samples of **a** Epoxy-C, **b** EPEMR20-C, **c** 1%MCC-C, **d** 3%MCC-C, and **e** 5%MCC-C



detachment from the EPEMR20 matrix. Notably, tensile properties improved for only up to 3% MCC, while impact strength improved up to 5% MCC. In MCC-filled EPEMR20-C, crack propagation deceleration may result from crack deviations caused by uniformly distributed, rigid MCC fillers, thereby enhancing impact strength.

Interlaminar shear strength (ILSS)

The investigation of interlaminar shear strength (ILSS) in the composite specimens aimed to clarify how the modification of the matrix by MCC fillers impacts the interface between fibers and the matrix. Figure 8 displays the ILSS versus displacement curve and ILSS for all bio-composites. Shear failure was the primary observed mode of failure. The results indicate that adding

20% EMR to epoxy composite increased ILSS by approximately 7.48%, likely due to better resin impregnation into the matrix facilitated by the lower viscosity of EPEMR20 resin. Notably, the highest interlaminar shear strength was achieved with 3 wt.% MCC-added flax fiber-reinforced EPEMR20-C, reaching 18.87 MPa. This marks a significant improvement of 14.25% and 22.7% compared to EPEMR20-C and Epoxy-C, respectively. The enhancement suggests that MCC particles inhibit fiber pull-out by forming chemical bonds with both the flax fiber and the matrix. The inclusion of MCC in the EPEMR20 matrix establishes chemical bonds with the fiber and matrix, aided by hydrogen and covalent bonding as discussed earlier. This interaction restricts filler and fabric layer movement within the matrix under external loads, thereby enhancing ILSS.

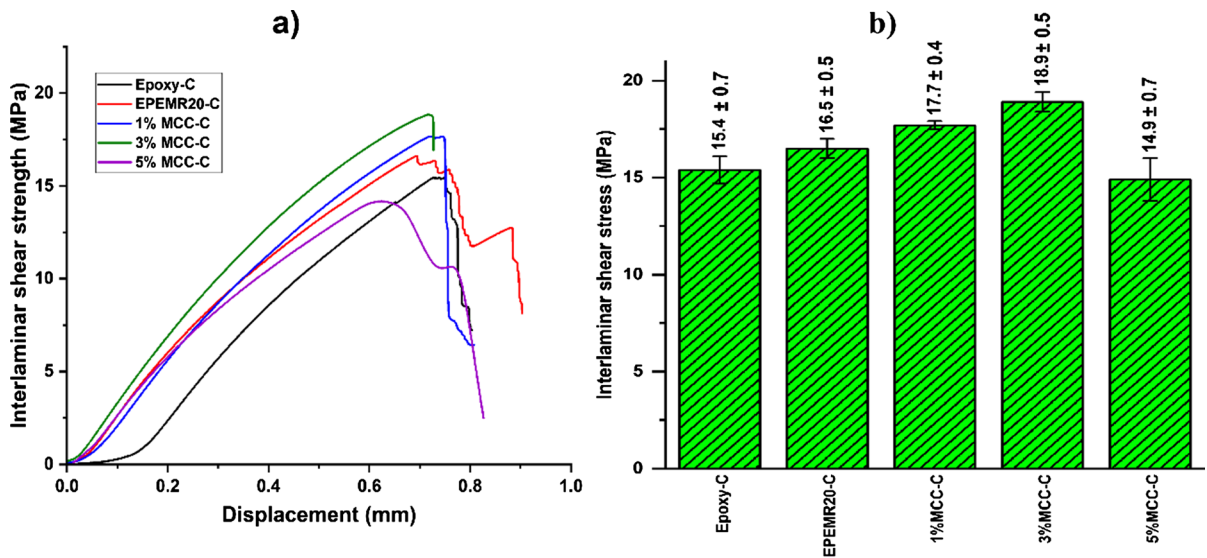


Fig. 8 **a** Inter-laminar shear strength versus displacement curve, and **b** ILSS for Epoxy-C, EPEMR20-C and its MCC modified composites

SEM morphology

Scanning electron microscopy was employed to gain insights into the failure analysis. Figure 9 displays the surface morphology of each composite that experienced damage during tensile testing. The SEM morphology of composite samples at lower magnifications exhibits typical failure characteristics, such as fibre breakage, fibre pull-out, fibre-matrix debonding, and fibre rupture. It is well documented that the strength of the composites appears to be significantly affected by the bonding occurring at the interface between the fibre and matrix (Sahoo et al. 2015c; Prasad et al. 2018; Sankar Lal et al. 2023). Among the bio-composites tested, the 3% MCC-C samples exhibited exceptional interfacial adhesion between fibers and the matrix, evidenced by the absence of fiber pull-outs. Conversely, the 5% MCC-C samples showed numerous voids and fiber pull-outs due to increased resin viscosity caused by higher MCC filler content (Fig. 9 i). To illustrate interfacial bonding, SEM images at higher magnifications are provided alongside lower magnification images. The fractured surface of Epoxy-C samples displayed a glassy appearance, signifying the inherent brittleness of the matrix material. This, combined with inadequate interfacial bonding due to higher epoxy resin viscosity, likely contributed to inferior

mechanical properties. In contrast, EPEMR20-C showed enhanced fiber adhesion at higher magnifications, credited to improved fiber wettability with less viscous epoxy/EMR resin, thus enhancing mechanical properties (Sankar Lal et al. 2023). The flax fibers exhibited a smooth surface upon failure in both the original epoxy and EMR-modified epoxy composites, as shown in Fig. 9 a) & b). Conversely, in the MCC-modified EPEMR20 composites, the fiber surfaces displayed signs of damage and showed adherence of MCC fillers and matrix fragments, indicating superior adhesion with the matrix system. This adhesion, possibly facilitated by hydrogen bonding between MCC filler and flax fiber, likely contributed to the enhanced mechanical properties by restraining fiber pullout during loading. The presence of voids on the fractured surface of 5% MCC-C (Fig. 9 i) suggests air entrapment due to increased viscosity, attributed to the higher MCC content. This elevated viscosity, in turn, leads to inferior interfacial adhesion, as depicted in Fig. 9 j).

Dynamic Mechanical Analysis (DMA)

DMA analysis offers insights into the viscoelastic properties of materials, evaluating parameters like storage modulus, loss modulus, and the loss factor across different temperature conditions and dynamic

Fig. 9 SEM morphology of tensile fractured surface at 200X for **a** Epoxy-C, **c** EPEMR20-C, **e** 1%MCC-C, **g** 3%MCC-C and **i** 5%MCC-C; and at 2kX for **b** Epoxy-C, **d** EPEMR20-C, **f** 1%MCC-C, **h** 3%MCC-C and **j** 5%MCC-C

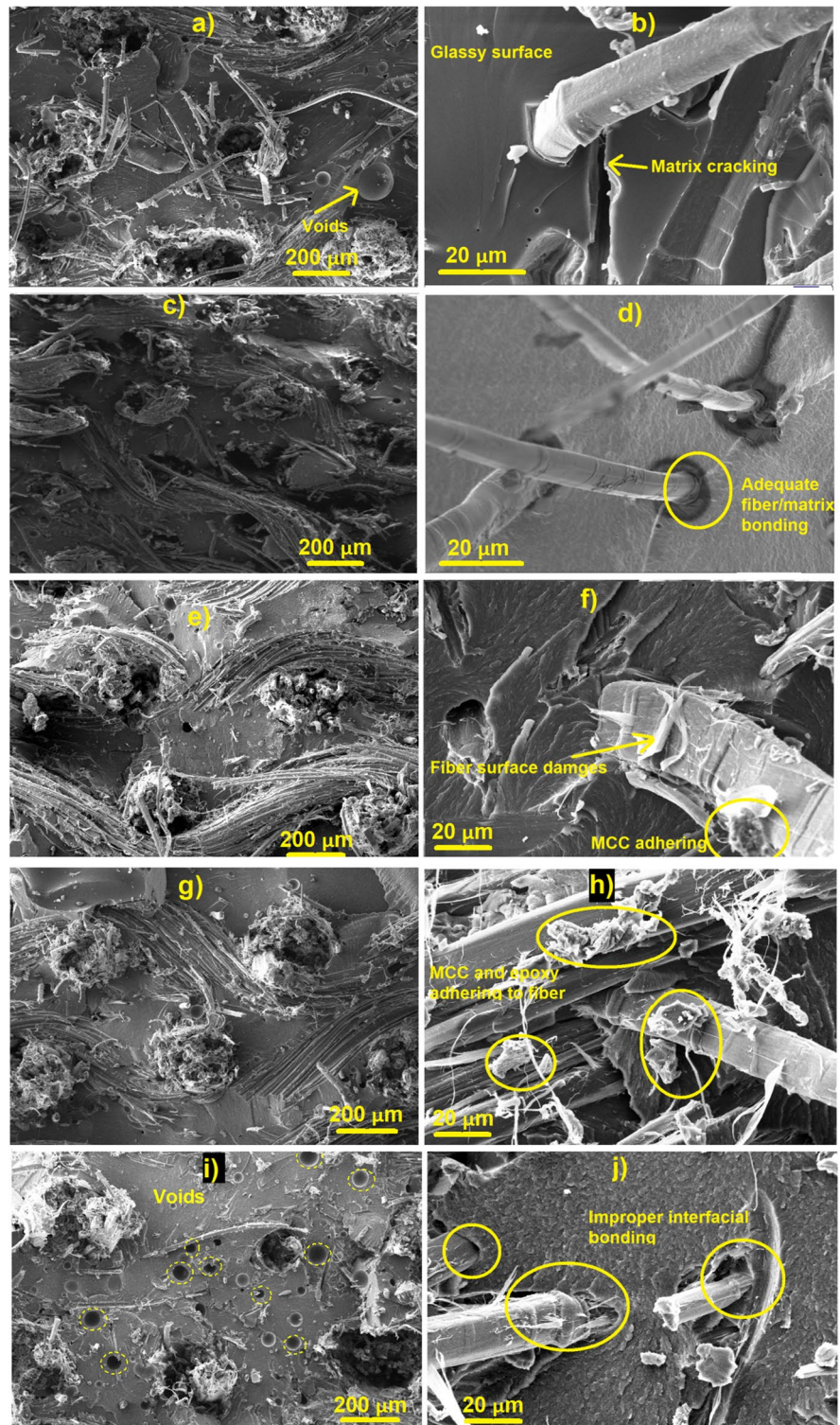
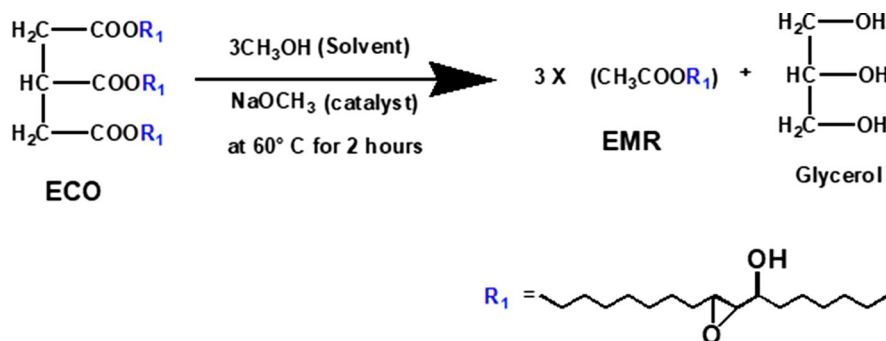


Table 1 Properties of reinforcement and resins provided by supplier

Raw materials	Properties	Values
Epoxy resin	Viscosity at 25 °C	9000–12000 mPa.s
	Mix viscosity at 25 °C	~ 1500 mPa.s
	Mix ratio with TETA (Resin: Hardener)	100: 10–12 by weight
	Epoxy content	185–189 g/mol
	Density at 25 °C	1.15 – 1.20 g/cm ³
	Tensile strength *	40 – 45 MPa
Hardener	Tensile modulus*	1900 – 2000 MPa
	Viscosity at 25 °C	~ 20 mPa.s
	Density at 25 °C	0.97 – 0.99 g/cm ³
	AHEW (Amine Hydrogen Equivalent Weight)	23 g/eq
ECO bio-resin	Viscosity at 25 °C*	5645 mPa.s
	Density at 25 °C	~ 1.05 g/ cm ³
	Epoxy content	450 – 455 g/eq
	Iodine value (gI/ 100 g)	10 max
EMR bio-resin	Viscosity at 25 °C*	544 mPa.s
	Density at 25 °C*	~ 0.97 g/cm ³
	Epoxy content*	485 – 487 g/eq
Flax fabric	Weave pattern	(0/90) plain weave
	Average thickness	0.38 mm
	Areal density	214 gsm
MCC filler	Particle size	≤ 25 μm
	Bulk density	1.55 g/cm ³

* Results obtained from our previous studies (Sankar lal et al. 2022b)

Scheme 1. EMR synthesis from ECO by base catalysed transesterification reaction**Table 2** Effect of MCC fillers on the tensile properties of EPEMR20-C bio-composites

Samples	Tensile strength (MPa)	Tensile modulus (MPa)	Elongation at break (%)
Epoxy-C	95.2 ± 3.7	1955.7 ± 41	7.45 ± 0.4
EPEMR20-C	101.3 ± 2.9	1865.1 ± 37	8.38 ± 0.3
1%MCC-C	105.7 ± 4.1	2450.9 ± 47	7.52 ± 0.2
3%MCC-C	113.2 ± 4.3	2611.7 ± 52	7.14 ± 0.3
5%MCC-C	90.7 ± 5.7	2349.7 ± 92	6.96 ± 0.4

loading. Figure 10 presents graphs depicting storage modulus, loss modulus, and tan delta for Epoxy-C, EPEMR20-C, and MCC-modified EPEMR20-C,

with corresponding viscoelastic properties listed in Table 3. As established earlier, the storage modulus (E') indicates a material's capacity to store external

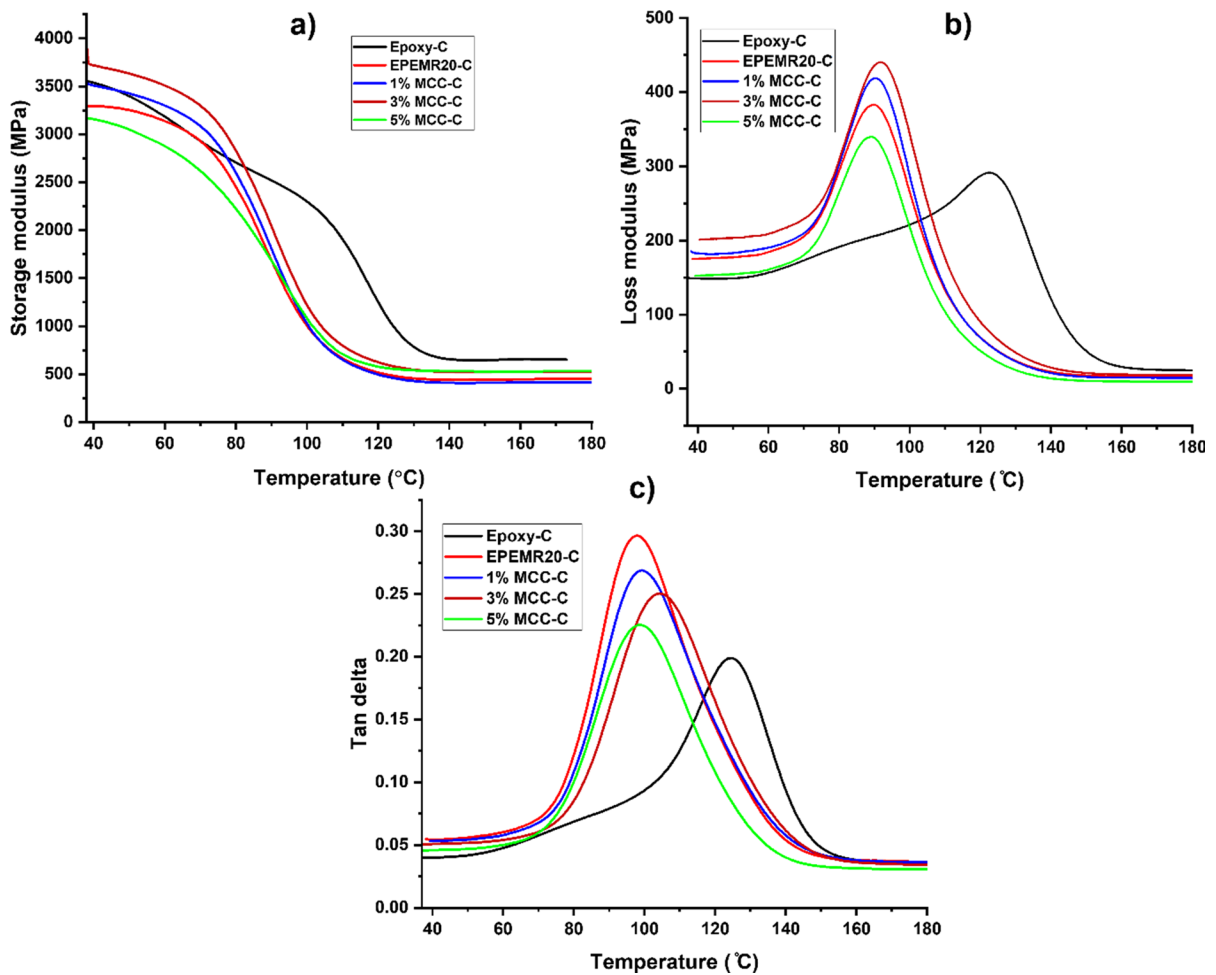


Fig. 10 Variation of **a)** Storage modulus, **b)** loss modulus, and **c)** tan delta with respect to temperature for bio-composites

force energy before experiencing permanent strain deformation. (Prasad et al. 2021). This parameter reflects the material's elasticity, signifying its rigidity and the stiffness of the polymeric structure. As shown in Fig. 10, E' values decrease with rising temperature, marking the material's transition from a glassy

to a rubbery state. At lower temperatures, the material is in a glassy state with dense packing and limited mobility, resulting in high E' values. With increasing temperature, intermolecular forces weaken, mobility enhances, and the packing arrangement becomes less rigid, leading to reduced E' values.

Table 3 Dynamic mechanical properties of Epoxy-C, EPEMR20-C and its MCC modified EPEMR20-C

Sample	Storage modulus (E'), MPa	Loss modulus (E''), MPa	Tan δ peak value	Glass transition temperature ($^{\circ}\text{C}$)
Epoxy-C	3562.4 ± 43	149.5 ± 11	0.1984 ± 0.01	124.3 ± 2
EPEMR20-C	3289.7 ± 34	174.7 ± 9	0.2962 ± 0.01	97.9 ± 1
1% MCC-C	3528.7 ± 23	185.3 ± 10	0.2688 ± 0.01	100.6 ± 3
3% MCC-C	3773.5 ± 27	202.5 ± 14	0.25 ± 0.01	105.4 ± 2
5% MCC-C	3178.2 ± 25	153.5 ± 11	0.225 ± 0.01	98.7 ± 1

Incorporating 20% of EMR into Epoxy-C resulted in a slight decrease (7%) in the storage modulus at room temperature (37 °C). This might be attributed to the fact that the base matrix of Epoxy-C contains a higher concentration of rigid aromatic groups, some of which are replaced by the aliphatic chains of EMR. The storage modulus of EPEMR20-C exhibits only a minor reduction, yet it remains comparable to that of the Epoxy composite, even with the inclusion of bio-resin's flexible chains. This is ascribed to the enhanced matrix-fibre bonding facilitated by the low viscosity of EPEMR20 (Sankar Lal et al. 2023). Nonetheless, there is an observed enhancement in the E' values (by 14.47%) as the MCC particle content increases to 3%, indicating its reinforcing effect at room temperature. This improvement can be attributed to both the MCC's ability to stiffen the matrix by restricting the mobility of the polymer molecules and also the enhanced bonding between flax fibres and the EPEMR20 matrix, which is facilitated by the even dispersion of MCC. The presence of MCC may aid in the formation of covalent bonds with the epoxy group and hydrogen bonding with the hydroxy groups of EMR and flax fibres, ultimately facilitating the formation of a resilient network. However, the Epoxy-C showed higher modulus at higher temperatures due to the higher content of rigid aromatic groups and higher crosslinking density. With further increase in the MCC content, the storage modulus decreased due to the formation of voids and inferior fibre/matrix bonding due to increased viscosity, as can be witnessed in SEM morphology.

The loss modulus (E'') measures the energy dissipation linked to polymer chain movement, affected by material viscosity. The " α " relaxation correlates with chain segment mobility within the polymer composite. E'' values increase with temperature until reaching a peak (Fig. 10 b)), indicating heightened chain mobility at higher temperatures. This increased movement generates molecular friction, dissipating force and elevating the loss modulus. Beyond the glass transition, molecular friction decreases, reducing energy dissipation and the loss modulus. Both at room and relaxation temperatures, the loss modulus increases proportionally, with the 3% MCC-C bio-composite exhibiting higher viscous dissipation than counterparts. This is due to restricted matrix chain movement at fiber surfaces. A higher loss modulus signifies enhanced interfacial interaction, reducing

polymer chain mobility. (Sahoo et al. 2015c). Also, the greater amount of heat dissipation is associated with increased internal friction, which is attributed to the enhanced interface development in the case of MCC-modified EPEMR20-C composites.

The loss factor, or $\tan \delta$, represents the ratio of a composite's loss modulus to its storage modulus, reflecting its energy-absorption capacity (Sankar Lal et al. 2022b; Sankar Lal et al. 2023). Figure 10 c) shows the variation of the loss factor with respect to temperature for all bio-composites. The intensity and the area beneath the $\tan \delta$ peak provide insights into the damping characteristics of the samples. Broader peaks typically suggest systems with heterogeneous structures, enabling significant viscous chain movements across various components over a wider temperature range (Sankar Lal et al. 2022a). The damping capacity of a composite material depends on the rigidity of the matrix and the interfacial bonding between fibre and the matrix. The stiffness imparted by the aromatic groups of epoxy might have resulted in a lower peak of $\tan \delta$ of Epoxy-C. Figure 10 c) reveals that EMR-modified epoxy composites have a larger area under the $\tan \delta$ curve compared to neat epoxy, indicating a higher proportion of elastomeric components. Introducing MCC reduces the peak height of the $\tan \delta$ curve, suggesting increased stiffness in the EPEMR20-C system. This stiffness enhancement is credited to MCC fillers' higher elastic modulus, enabling them to withstand greater loads and induce less strain at the interface during testing (Sankar and Sekar 2023). Moreover, the decrease in $\tan \delta$ peak intensity is attributed to improved adhesion between fibers and the matrix in MCC-filled EPEMR20-C, as explained previously. It is well documented that composites with weak interfacial bonding between fibers and the matrix demonstrate higher energy dissipation, indicated by a more pronounced $\tan \delta$ peak, unlike composites with a well-bonded interface (Sahoo et al. 2018b; Senthilkumar et al. 2021; Sankar Lal et al. 2023).

The glass transition temperature (T_g) of the composite systems was identified by locating the peak on the $\tan \delta$ curve. Epoxy-C showed the highest T_g among the tested samples, attributed to its higher content of rigid aromatic groups and greater crosslinking density. Interestingly, THE addition of MCC to EPEMR20-C resulted in an increased T_g , suggesting enhanced stiffness of the EPEMR20 matrix

and improved interfacial bonding, as detailed in the mechanical characterization section.

Drop weight impact test

The effect of EMR and MCC on the impact behaviour of the fabric reinforced epoxy composites in terms of the peak load, maximum deflection, impact energy, elastic and absorbed energy was analysed. To assess the damage caused by impacts on composites, it is typical to consider absorbed energy (E_a) and impact energy (E_i). Impact energy represents the kinetic energy of the impactor striking the samples just before contact, while absorbed energy accounts for the energy dissipated within the system by various mechanisms that occur after contact with the object. These mechanisms include friction, elastic and plastic deformation, and notably, those specific to the material itself, such as de-bonding, delamination, matrix cracking fibre breakage, and pull-out (Sarasini et al. 2014; Scarponi et al. 2016).

Impact force—displacement

The correlation between contact force and displacement serves as a crucial metric for understanding a material's response to impact forces (Wang et al. 2021c). The displacement on the graph illustrates both the motion of the impactor and the deformation of the impacted sample as they come into contact. Atas and Sayman (2008) introduced two categories of force–displacement curves, namely 'closed' and 'open,' which correspond to scenarios involving non-perforated and perforated composite systems subjected to impact loading. The force–displacement curve can typically be segmented into three zones

labelled as I, II, and III, as illustrated in Fig. 11 a). Zone I represents the elastic behaviour of the specimen until the force reaches the threshold for initiating damage. Here, laminate failure begins with matrix cracking and initial delamination. In zone II, damage progresses as the impactor penetrates the composite laminate until reaching a complete stop, marking the turning point. The force fluctuations in this area indicate damage to both fiber and matrix within the plies, suggesting the spread of damage. In general, a broader Zone II typically signals more extensive damage throughout the laminate, resulting in a larger overall damaged area. For non-perforating impacts, Zone III marks the phase where the force diminishes as the impactor rebounds due to the laminate's stored elastic energy, ultimately leading to full rebound because of the composite laminate's elastic resilience. The deflection observed at the end of Zone III indicates permanent deformation of the plate. However, in high-energy impacts like perforation tests, Zone III is replaced by a sudden decrease in force without any strain recovery, as the impactor fully penetrates the material (Ravandi et al. 2017). Additionally, an extra Zone IV, marked by a horizontal wavy line (Fig. 11b)), is noted in perforated tests. This zone arises from friction between the impactor and the wall of the perforated hole after penetration of the specimen. To evaluate energy absorption and impact response, drop weight impact tests were conducted at two energy levels for all bio-composite panels. Non-perforated and perforated impact tests on composite samples were performed by impacting with a 10 J and 20 J impactor, respectively.

All three bio-composites exhibited a similar curve pattern symbolizing similar failure modes at the respective levels of impact energy as depicted in

Fig. 11 Impact force versus deformation curve under LVI test for Epoxy-C, EPEMR20-C and 3% MCC-C at **a** 10 J, and **b** 20 J

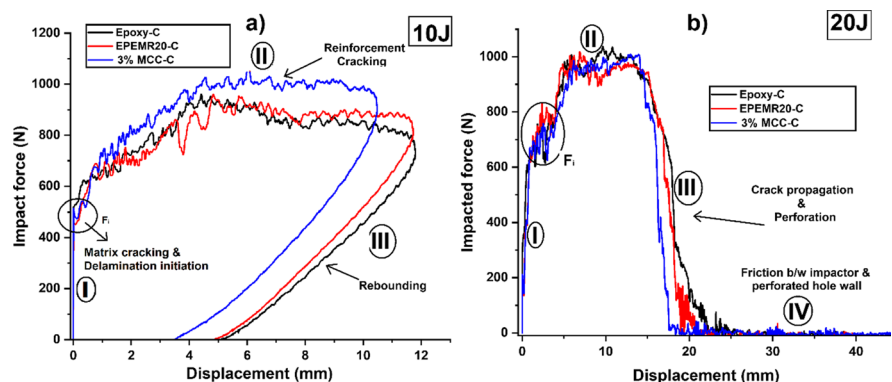


Fig. 12. Upon exposure to 10 J and 20 J impacts, the composites developed cracks and a perforated hole, respectively. To quantify the extent of damage, the total crack length (sum of longitudinal and transverse components) for the 10 J impact and the area of the perforated hole for the 20 J impact were analyzed using Digimizer software, as outlined in Table 4. Notably, the damage observed on the back side of the composite laminate was more pronounced compared to the front side, suggesting delamination as a primary failure mechanism (Sevkat et al. 2009; Sarasini et al. 2014; Matadi Boubimba et al. 2015; Umair

et al. 2021). While this damage mode is prevalent, it's not assumed to be the only one. Interfacial failures like de-bonding and pull-out are anticipated to be significant. The least difference in damage between the front and back faces of laminate was observed in 3% MCC-C laminates, indicating superior inter-laminar and interfacial adhesion, as discussed earlier. Therefore, it's inferred that incorporating EMR and MCC into the epoxy composite reduces both crack length and damaged area. Notably, the inclusion of EMR in the epoxy composite led to an increase in maximum impact force (F_{Max}), which was further enhanced with

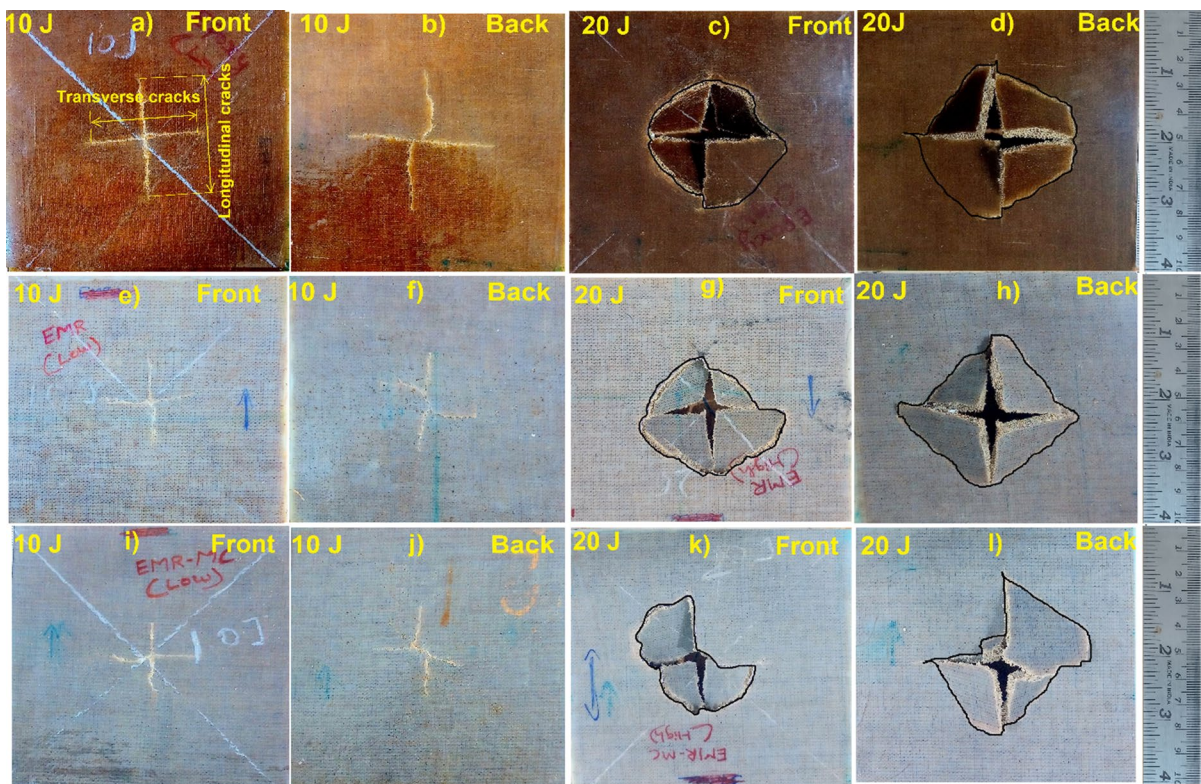


Fig. 12 Digital images of the evolution of damage on the front and rear surfaces of **a-d** Epoxy-C, **e-h** EPEMR20-C, and **i-l** 3% MCC-C subjected to impacts at 10 J and 20 J

Table 4 Damage quantification of composites subjected to impacts at 10 J and 20 J in LVI test

Sample	Total crack length (mm)		Damage area (mm ²)	
	10 J	20 J	Front side	Back side
Epoxy-C	77.63 ± 2.2	110.36 ± 3.7	1057.4 ± 23	1421.2 ± 23
EPEMR20-C	61.61 ± 3.4	79.31 ± 2.7	927.23 ± 27	1274.5 ± 34
3% MCC-C	61.43 ± 2.5	64.81 ± 2.5	679.34 ± 19	997.2 ± 27

the addition of 3% MCC to the EPEMR20-C for both impact energy levels (Table 5). This could be attributed to the improvement in adhesion between the fibre and the matrix as a result of the reduced viscosity of EPEMR20 resin system (Sankar Lal et al. 2023). The introduction of MCC filler into the EPEMR20 resin system potentially leads to the formation of hydrogen bonds between MCC fillers, flax fibers, and EMR, facilitated by their hydroxy groups. This enhanced interfacial bonding, supported by SEM morphology analysis (Fig. 9), contributed to the highest resistance to impact damage observed in EMR-modified MCC-filled bio-composites. Additionally, EPEMR20-C exhibited the least displacement among MCC-filled composites, indicating its superior stiffness. Marrot et al. (2014) conducted a thorough multi-scale examination of the adhesion between flax fibres and commercially available epoxy and polyester matrices. The de-bonding tests revealed satisfactory adhesion at the microscopic level for each composite. Moreover, they observed favorable mechanical outcomes when utilizing partially biobased polyester and epoxy resins in natural fiber-reinforced composites. In particular, the significance of the high hydroxy group content in the amine hardener was highlighted as partially explaining the substantial adhesion observed for the fibre/bioepoxy combination. Because hydroxy groups are present on MCC, flax fibre, and EMR, this also applies to the current situation.

Absorbed energy-time response

Analysing the dynamic behaviour of composites relies significantly on the measurement of energy absorption during impact (Wang et al. 2021a). The absorbed energy by the composite specimen

can be characterized by the area under the contact force–displacement curve. As a result, the energy absorption value can be calculated by integrating the force–displacement curve resulting from the impact, utilizing the approach outlined in Eq. 4:

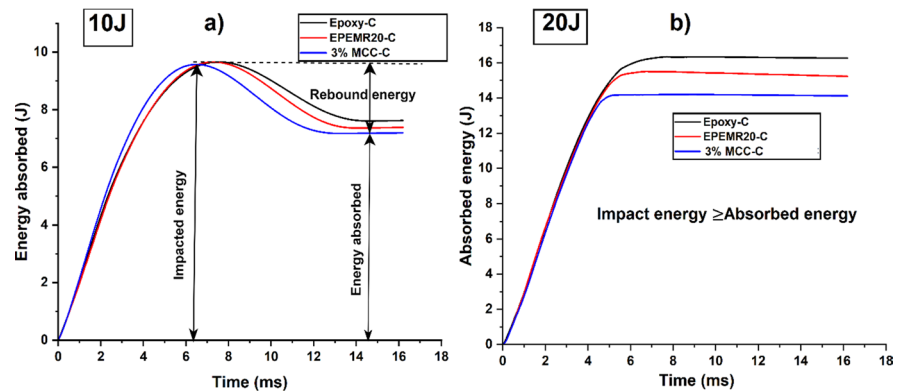
$$E_{\text{absorbed energy}} = \int F(\delta)d\delta \quad (4)$$

Here, ‘ $E_{\text{absorbed energy}}$ ’ denotes the absorbed energy, ‘ $F(\delta)$ ’ represents the relationship between contact force and displacement, and ‘ δ ’ indicates the displacement. Elastic energy is characterized as the portion of the impact energy that gets transmitted to the specimen and becomes stored within it. Subsequently, this stored energy is later released to the impactor, playing a crucial role in the impactor’s rebound. On the other hand, absorbed energy refers to the fraction of the impact energy that the specimen absorbs in order to undergo damage. As there is no penetration in a scenario involving rebound, a portion of the energy is gradually regained, stabilizing at a constant level while unloading, till the moment when the impactor separates from the specimen’s surface and rebounds. The flat line in Fig. 13 a) represents the conclusion of the impact event and signifies the absorbed energy. In this impact scenario, delamination might play the most significant role in contributing to the absorbed energy, which is consistent with previous research (Scarponi et al. 2016; Umair et al. 2021; Wang et al. 2021b, a). The rebounding impactor recovers some of the initial energy as elastic energy, leading to a decrease in the final energy absorbed compared to the initial impact energy. The rebounding impactor retrieves elastic energy, which is the difference between the maximum energy and the absorbed energy.

Table 5 Parameters obtained from low velocity impact test for different composites

Impact energy (J)	Sample	Peak force (N)	Contact duration (ms)	Max. deformation (mm)	Energy absorbed (J)
10 J	Epoxy-C	959.1 ± 32	14.65 ± 1.1	11.8 ± 0.4	7.65 ± 0.3
	EPEMR20-C	972.7 ± 27	14.02 ± 1	11.52 ± 0.3	7.37 ± 0.2
	3%MCC -C	1057.7 ± 37	13.07 ± 0.9	10.47 ± 0.4	7.19 ± 0.5
20 J	Epoxy-C	1009.4 ± 41	7.73 ± 0.4	-	16.34 ± 0.9
	EPEMR20-C	1017.5 ± 31	6.59 ± 0.5	-	15.23 ± 0.7
	3%MCC-C	1049.7 ± 27	5.22 ± 0.3	-	14.15 ± 1.1

Fig. 13 Energy absorption under LVI test for Epoxy-C, EPEMR20-C and 3% MCC—C at **a** 10 J, and **b** 20 J



In Fig. 13 a), the observed absorbed energy indicated that the total impact energy did not match the absorbed energy, suggesting that there was no penetration but rather a rebound. In the context of impact situations, delamination stands out as the primary factor influencing the amount of absorbed energy, in agreement with earlier studies (Sevkat et al. 2009; Sarasini et al. 2014; Matadi Boumbimba et al. 2015; Wang et al. 2021b). Furthermore, the inclusion of nano and micro-fillers has been shown to boost inter-laminar shear strength, consequently increasing resistance to delamination (Nor et al. 2019). Hence, altering the resin system by incorporating MCC fillers results in a reduction of impact damage due to decreased energy absorption.

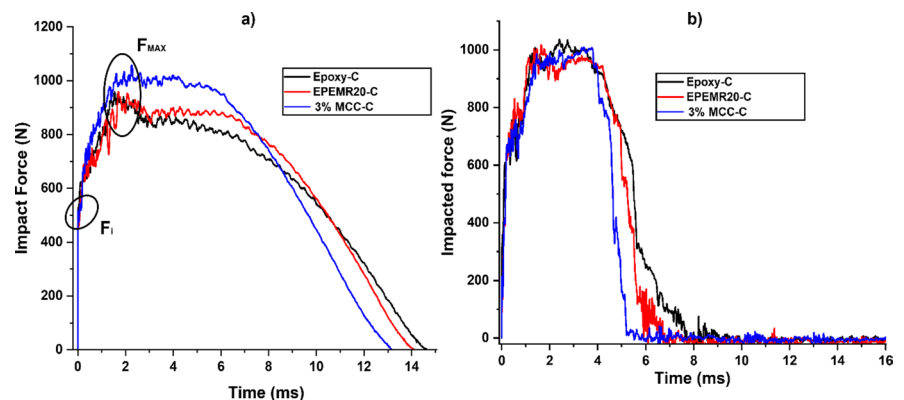
When the impactor penetrates the specimen, resulting in an open-type force–displacement curve, the initial impact energy equals or surpasses the energy absorbed by the composite. Even after penetrating the composite, the impactor retains some kinetic energy. Figure 13 clearly demonstrates that the impact energy

plays a significant role and exerts a substantial influence on the response of materials during impacts (Wang et al. 2021a). The absorbed energy, indicating the energy transferred from the impactor to the composite specimens at the end of impact events, increases with higher impact energy, as depicted. This rise in absorbed energy corresponds to more severe damage to the composite, underscoring the correlation between impact energy and material response observed in Fig. 12.

Impact force–time response

Figure 14 depicts the force–time responses of Epoxy-C, EPEMR20-C, and 3% MCC-C under various low-velocity drop weight impacts. These plots aid in identifying the maximum force indicative of impact damage resistance. The peak force represents the maximum force the specimen can endure at a specific energy level along the force versus time curves. Initially, in the elastic range, the impact force sharply

Fig. 14 Typical Impact force vs. time response for composites at **a** 10 J, and **b** 20 J



risers linearly until reaching a specific force denoted as ' F_i ' marking the onset of damage and a change in stiffness. F_i serves as an indicator of the laminate's ability to withstand initial damage, with a subsequent decrease in slope symbolizing reduced stiffness due to damage initiation. Beyond ' F_i ' changes in impact force signify the progression of damage within the composite laminates. Following initial failure, the load-time curve fluctuates as it ascends, eventually reaching its maximum threshold force (F_{Max}) before gradually declining, particularly for low impact energy levels and suddenly for high energy levels. Notably, F_{Max} tends to be slightly higher for composites based on EPEMR20, with further increases observed upon adding 3% MCC.

Additionally, as shown in Fig. 14, it's clear that the impact durations for composites with 20% EMR in epoxy were significantly shorter compared to neat epoxy composites, regardless of the impact energy levels. Furthermore, this duration was further decreased with the addition of 3% MCC into EPEMR20-C. The difference in impact durations can be attributed to the improved adhesion between fibers and the matrix in composites with MCC incorporation, as observed from SEM morphology.

Conclusion

The present study systematically investigates the impact of incorporating a rigid MCC filler into flax fibre-reinforced EMR toughened epoxy composites. The mechanical, dynamic mechanical, and low-velocity impact responses of these composites were analysed to assess the impact of the MCC filler. Based on the results collected, the following conclusions can be made.

- Incorporating MCC into EPEMR20-C not only restored the lost modulus due to EMR addition to Epoxy-C but also enriched the tensile modulus up to 34%, attributed to the stiffening effect of MCC and the establishment of hydrogen bonding among the hydroxy groups in MCC, flax fibre, and EMR, resulting in a resilient network.
- The mechanical properties like tensile, impact, and inter-laminar shear strength values improved by 19%, 34.2%, and 22.7%, respectively for MCC filled composites as compared to Epoxy-C.

- The addition of MCC led to enhancements in both storage and loss moduli, with a corresponding rise of 14.47% and 15.8%.
- The SEM analysis showed that the fibre surface of MCC-modified EPEMR20 composites displays surface damage, with MCC fillers and matrix fragments adhering, suggesting enhanced adhesion to the matrix system.
- In LVI testing, the inclusion of MCC led to lower energy absorption compared to both the neat and EMR-modified epoxy composites, consequently reducing physical damage. Moreover, composite laminates with MCCs exhibited increased peak force and the least damage attributed to an enhanced fibre/matrix interface.

The results imply that these sustainable bio-composites, modified with bio-resin and bio-filler exhibiting enhanced mechanical performance, have the potential to substitute petroleum-based epoxy composites in structural applications.

Authorship contribution

Sathyaraj Sankaral- Conceptualization, Methodology, Investigation, Characterizing the samples, writing – original draft, Validation, Formal analysis, Writing—review & editing. **Sekar Kannan-** Resources, Writing—review & editing, Supervision.

Acknowledgments The author, Sathyaraj Sankaral, expresses gratitude to the National Institute of Technology, Calicut, Kerala, India, for providing the scholarship, contingency, TEQIP, and Plan Fund research grant that facilitated the execution of this research work. Special thanks are extended to Dr. M. L. Joy, Professor and Head of the Department of Mechanical Engineering at NIT Calicut, and Dr. Sushant Kumar Sahoo of CSIR NIIST for their unwavering support throughout the research. A special thanks to Dr. V. Arumugam, Professor, Department of Aerospace Engg, Madras Institute of Technology, Chennai for providing facility to conduct LVI Test.

Author contributions Sathyaraj Sankaral- Conceptualization, Methodology, Investigation, Characterizing the samples, writing – original draft, Validation, Formal analysis, Writing - review & editing. Sekar Kannan- Resources, Writing - review & editing, Supervision.

Funding The authors did not receive support from any organization for the submitted work.

Data availability The datasets generated during and/or analysed during the current study are available from the corresponding author on reasonable request.

Declarations

Competing interest The authors declare that they have no known competing financial interests or personal relationships that could have appeared to influence the work reported in this paper.

References

- Ansari F, Lindh EL, Furo I, Johansson MKG, Berglund LA (2016) Interface tailoring through covalent hydroxy-epoxy bonds improves hygromechanical stability in nanocellulose materials. *Compos Sci Technol* 134:175–183. <https://doi.org/10.1016/j.compscitech.2016.08.002>
- Atas C, Sayman O (2008) An overall view on impact response of woven fabric composite plates. *Compos Struct* 82:336–345. <https://doi.org/10.1016/j.compstruct.2007.01.014>
- Di Mauro C, Genua A, Rymarczyk M, Dobbels C, Malburet S, Graillot A, Mija A (2021) Chemical and mechanical reprocessed resins and bio-composites based on five epoxidized vegetable oils thermosets reinforced with flax fibers or PLA woven. *Compos Sci Technol* 205:108678. <https://doi.org/10.1016/j.compscitech.2021.108678>
- Fu Q, Tan J, Han C, Zhang X, Fu B, Wang F, Zhu X (2020) Synthesis and curing properties of castor oil-based triglycidyl ether epoxy resin. *Polym Adv Technol* 31:2552–2560. <https://doi.org/10.1002/pat.4982>
- Jabbar A, Militký J, Wiener J, Kale BM, Ali U, Rwawiire S (2017) Nanocellulose coated woven jute/green epoxy composites: Characterization of mechanical and dynamic mechanical behavior. *Compos Struct* 161:340–349. <https://doi.org/10.1016/j.compstruct.2016.11.062>
- Kannan S, Sankar Lal S (2023) Effect of Plant Oil Derived Bio-Resin and Curing Temperature on Static and Dynamic Mechanical Properties of Epoxy Network. *J Biomimetics, Biomater Biomed Eng* 63:147–156. <https://doi.org/10.4028/p-ui9jks>
- Kerche EF, da Silva VD, Fonseca E, Salles NA, Schrekker HS, Amico SC (2021) Epoxy-based composites reinforced with imidazolium ionic liquid-treated aramid pulp. *Polymer (Guildf)* 226. <https://doi.org/10.1016/j.polymer.2021.123787>
- Kumar S, Samal SK, Mohanty S, Nayak SK (2018) Bio-based tri-functional epoxy resin (TEEA) blend cured with anhydride (MHHPA) based cross-linker: Thermal, mechanical and morphological characterization. *J Macromol Sci Part A Pure Appl Chem* 55:496–506. <https://doi.org/10.1080/10601325.2018.1470468>
- Mahboob Z, El Sawi I, Zdero R, Fawaz Z, Bougherara H (2017) Tensile and compressive damaged response in Flax fibre reinforced epoxy composites. *Compos Part A Appl Sci Manuf* 92:118–133. <https://doi.org/10.1016/j.compositesa.2016.11.007>
- Marrot L, Bourmaud A, Bono P, Baley C (2014) Multi-scale study of the adhesion between flax fibers and biobased thermoset matrices. *Mater Des* 62:47–56. <https://doi.org/10.1016/j.matdes.2014.04.087>
- Matadi Boumbimba R, Froustey C, Viot P, Gerard P (2015) Low velocity impact response and damage of laminate composite glass fibre/epoxy based tri-block copolymer. *Compos Part B Eng* 76:332–342. <https://doi.org/10.1016/j.compositesb.2015.02.007>
- Motta Neves R, Zattera AJ, Campos Amico S (2021) Enhancing thermal and dynamic-mechanical properties of epoxy reinforced by amino-functionalized microcrystalline cellulose. *J Appl Polym Sci* 138:1–11. <https://doi.org/10.1002/app.51329>
- Nascimento NRD, Pinheiro IF, Alves GF, Mei LHI, Macedo Neto JCD, Morales AR (2021) Role of cellulose nanocrystals in epoxy-based nanocomposites: mechanical properties morphology and thermal behavior. *Polímeros* 31(3). <https://doi.org/10.1590/0104-1428.20210057>
- Neves RM, Ornaghi HL, Zattera AJ, Amico SC (2020) The influence of silane surface modification on microcrystalline cellulose characteristics. *Carbohydr Polym* 230. <https://doi.org/10.1016/j.carbpol.2019.115595>
- Nor AFM, Sultan MTH, Jawaid M, Azmi AMR, Shah AUM (2019) Analysing impact properties of CNT filled bamboo/glass hybrid nanocomposites through drop-weight impact testing, UWPI and compression-after-impact behaviour. *Compos Part B Eng* 168:166–174. <https://doi.org/10.1016/j.compositesb.2018.12.061>
- Paluvai NR, Mohanty S, Nayak SK (2015) Fabrication and evaluation of acrylated epoxidized castor oil-toughened diglycidyl ether of bisphenol A nanocomposites. *Can J Chem Eng* 93:2107–2116. <https://doi.org/10.1002/cjce.22320>
- Parveen S, Rana S, Fanguero R, Paiva MC (2017) A novel approach of developing micro crystalline cellulose reinforced cementitious composites with enhanced microstructure and mechanical performance. *Cem Concr Compos* 78:146–161. <https://doi.org/10.1016/j.cemconcomp.2017.01.004>
- Pichandi S, Rana S, Parveen S, Fanguero R (2018) A green approach of improving interface and performance of plant fibre composites using microcrystalline cellulose. *Carbohydr Polym* 197:137–146. <https://doi.org/10.1016/j.carbpol.2018.05.074>
- Prasad V, Joseph MA, Sekar K (2018) Investigation of mechanical, thermal and water absorption properties of flax fibre reinforced epoxy composite with nano TiO₂ addition. *Compos Part A* 115:360–370. <https://doi.org/10.1016/j.compositesa.2018.09.031>
- Prasad V, Sekar K, Varghese S, Joseph MA (2020) Evaluation of interlaminar fracture toughness and dynamic mechanical properties of nano TiO₂ coated flax fibre epoxy composites. *Polym Test* 91:106784. <https://doi.org/10.1016/j.polymertesting.2020.106784>
- Prasad V, Sekar K, Joseph MA (2021) Mechanical and water absorption properties of nano TiO₂ coated flax fibre epoxy composites. *Constr Build Mater* 284:122803. <https://doi.org/10.1016/j.conbuildmat.2021.122803>
- Ramesh P, Prasad BD, Narayana KL (2020) Effect of MMT Clay on Mechanical, Thermal and Barrier Properties

- of Treated Aloe vera Fiber/ PLA-Hybrid Biocomposites. *SILICON* 12:1751–1760. <https://doi.org/10.1007/s12633-019-00275-6>
- Ravandi M, Teo WS, Tran LQN, Yong MS, Tay TE (2017) Low velocity impact performance of stitched flax/epoxy composite laminates. *Compos Part B Eng* 117:89–100. <https://doi.org/10.1016/j.compositesb.2017.02.003>
- Rehman MM, Zeeshan M, Shaker K, Nawab Y (2019) Effect of micro-crystalline cellulose particles on mechanical properties of alkaline treated jute fabric reinforced green epoxy composite. *Cellulose* 26:9057–9069. <https://doi.org/10.1007/s10570-019-02679-4>
- Sahoo SK, Mohanty S, Nayak SK (2015b) Toughened bio-based epoxy blend network modified with transesterified epoxidized soybean oil: Synthesis and characterization. *RSC Adv* 5:13674–13691. <https://doi.org/10.1039/c4ra11965g>
- Sahoo SK, Khandelwal V, Manik G (2018a) Renewable Approach to Synthesize Highly Toughened Bioepoxy from Castor Oil Derivative-Epoxy Methyl Ricinoleate and Cured with Biorenewable Phenalkamine. *Ind Eng Chem Res* 57:11323–11334. <https://doi.org/10.1021/acs.iecr.8b02043>
- Sahoo SK, Khandelwal V, Manik G (2018b) Influence of epoxidized linseed oil and sisal fibers on structure–property relationship of epoxy biocomposite. *Polym Compos* 39:E2595–E2605. <https://doi.org/10.1002/pc.24857>
- Sahoo SK, Mohanty S, Nayak SK (2015a) Synthesis and characterization of bio-based epoxy blends from renewable resource based epoxidized soybean oil as reactive diluent. *Chinese J Polym Sci (English Ed)* 33:137–152. <https://doi.org/10.1007/s10118-015-1568-4>
- Sahoo SK, Mohanty S, Nayak SK (2015c) Study on the effect of woven sisal fiber mat on mechanical and viscoelastic properties of petroleum based epoxy and bioresin modified toughened epoxy network. *J Appl Polym Sci* 132. <https://doi.org/10.1002/app.42699>
- Sankar Lal S, Kannan S, Sahoo SK (2022a) Influence of flax fiber orientation on mechanical, thermo-mechanical and interfacial adhesion properties of epoxidized methyl ricinoleate modified epoxy composite: A sustainable green composite for cleaner production. *Mater Today Commun* 33:104648. <https://doi.org/10.1016/j.mtcomm.2022.104648>
- Sankar Lal S, Sahoo SK, Kannan S (2022b) Investigation on curing kinetics, water diffusion kinetics and thermo-mechanical properties of functionalized castor oil based epoxy copolymers. *J Polym Res* 29:275. <https://doi.org/10.1007/s10965-022-03122-2>
- Sankar S, Sekar L (2023) Influence of Microcrystalline Cellulose on Curing Kinetics, Mechanical and Thermo-Mechanical Properties of Epoxy Methyl Ricinoleate Toughened Epoxy Copolymer. *J Polym Environ*. <https://doi.org/10.1007/s10924-023-03046-y>
- Sankar Lal S, Kannan S, Sahoo SK (2023) Investigation on the effect of castor-oil based bio-resins on mechanical, viscoelastic, and water diffusion properties of flax fiber reinforced epoxy composites. *Polym Compos* 4289–4308. <https://doi.org/10.1002/pc.27410>
- Sarasini F, Tirillò J, Ferrante L, Valente M, Valente T, Lampani L, Gaudenzi P, Cioffi S, Iannace S, Sorrentino L (2014) Drop-weight impact behaviour of woven hybrid basalt-carbon/epoxy composites. *Compos Part B Eng* 59:204–220. <https://doi.org/10.1016/j.compositesb.2013.12.006>
- Scarponi C, Sarasini F, Tirillò J, Lampani L, Valente T, Gaudenzi P (2016) Low-velocity impact behaviour of hemp fibre reinforced bio-based epoxy laminates. *Compos Part B Eng* 91:162–168. <https://doi.org/10.1016/j.compositesb.2016.01.048>
- Senthilkumar K, Saba N, Chandrasekar M, Jawaid M, Rajini N, Siengchin S, Ayrilmis N, Mohammad F, Al-Lohedan HA (2021) Compressive, dynamic and thermo-mechanical properties of cellulosic pineapple leaf fibre/polyester composites: Influence of alkali treatment on adhesion. *Int J Adhes Adhes* 106:102823. <https://doi.org/10.1016/j.ijadhadh.2021.102823>
- Sevkat E, Liaw B, Delale F, Raju BB (2009) Drop-weight impact of plain-woven hybrid glass-graphite/toughened epoxy composites. *Compos Part A Appl Sci Manuf* 40:1090–1110. <https://doi.org/10.1016/j.compositesa.2009.04.028>
- Stanley WF, Bandaru AK, Rana S, Parveen S, Pichandi S (2021) Mechanical, dynamic-mechanical and wear performance of novel non-crimp glass fabric-reinforced liquid thermoplastic composites filled with cellulose microcrystals. *Mater Des* 212:110276. <https://doi.org/10.1016/j.matdes.2021.110276>
- Sudha GS, Kalita H, Mohanty S, Nayak SK (2017a) Biobased epoxy/carbon fiber composites: Effect on mechanical, thermo-mechanical and morphological properties. *J Macromol Sci Part A Pure Appl Chem* 54:756–764. <https://doi.org/10.1080/10601325.2017.1332466>
- Sudha GS, Kalita H, Mohanty S, Nayak SK (2017b) Castor oil modified by epoxidation, transesterification, and acrylation processes: Spectroscopic characteristics. *Int J Polym Anal Charact* 22:519–525. <https://doi.org/10.1080/1023666X.2017.1334171>
- Umair M, Hussain M, Abbas Z, Shaker K, Nawab Y (2021) Effect of weave architecture and glass microspheres percentage on the low velocity impact response of hemp/green epoxy composites. *J Compos Mater* 55:2179–2195. <https://doi.org/10.1177/0021998320987605>
- Wang C, Ramakrishnan KR, Shankar K, Morozov E, Wang H, Fien A (2021a) Homogenized shell element-based modeling of low-velocity impact response of stainless-steel wire mesh. *Mech Adv Mater Struct* 28:1932–1947. <https://doi.org/10.1080/15376494.2020.1716415>
- Wang C, Su D, Xie Z, Zhang K, Wu N, Han M, Zhou M (2021b) Low-velocity impact response of 3D woven hybrid epoxy composites with carbon and heterocyclic aramid fibres. *Polym Test* 101:107314. <https://doi.org/10.1016/j.polymertesting.2021.107314>
- Wang C, Wang H, Shankar K, Morozov EV, Hazell PJ (2021c) On the mechanical behaviour of steel wire mesh subjected to low-velocity impact. *Thin-Walled Struct* 159:107281. <https://doi.org/10.1016/j.tws.2020.107281>

Publisher's Note Springer Nature remains neutral with regard to jurisdictional claims in published maps and institutional affiliations.

Springer Nature or its licensor (e.g. a society or other partner)

holds exclusive rights to this article under a publishing agreement with the author(s) or other rightsholder(s); author self-archiving of the accepted manuscript version of this article

is solely governed by the terms of such publishing agreement and applicable law.